Computational Models of Trajectory Investigation of Marine Geophysical Fields and Its Implementation for Solving Problems of Map-Aided Navigation

L.V. Kiselev [1*], V.B. Kostousov [2], A.V.Medvedev[1], A.E. Tarkhanov[2],

K.V. Dunaevskaya[2]

[1] *IMTP FEB RAS, Vladivostok, Russia*

E-mail: imtp@marine.febras.ru

[2] *IMM UB RAS, Ekaterinburg, Russia*

E-mail: dir-info@imm.uran.ru

Abstract: Comprehensive investigations of geophysical fields (GPF) of the ocean are among the top priority problems in underwater robotics. Problems reside in developing automated systems capable of real-time operation for gathering, accumulating, and processing diverse geophysical information. The data's total volume is applied for long-term or real-time monitoring of marine areas, environment or objects surveillance, mapping certain regions, or anomalies in geographical coordinates. One of the main elements of such systems is the computational models sensitive to properties of geophysical fields, features of search routes of underwater vehicles, and particular aspects of missions performed during trajectory measurements and features of navigational support tasks. The work considers computational models of comprehensive interpretation of the results of trajectory measurements of geophysical fields using an autonomous underwater vehicle (AUV), and estimation of accuracy of map-aided navigation on the reconstructed map of geophysical fields. Algorithms and software consider distinctive features of representation of bathymetry, magnetometry, and gravimetry data visualized in 2D and 3D. Algorithm of map-aided navigation by the reconstructed fields is discussed. The final assessments of the considered models' accuracy consider averaged errors of measurements, mapping, and inertial navigation. Obtained assessments are based on theoretical investigations, results of model experiments, and experimental trials of AUV's systems under actual operating conditions.

Keywords: autonomous underwater robot (autonomous unmanned underwater vehicle), motion control, navigation, marine geophysical fields, trajectory measurements, mapping, computational models, bathymetry, magnetometry, gravimetry.

1. INTRODUCTION

Nowadays, geophysical measurements using aerospace, ground, and marine means are widely used for precise navigation of moving objects and investigation of the Earth's geological structure. Particular importance is attached to comprehensive research of anomalous fields in different regions of the Earth's surface, including aquatic areas promising in terms of its geological structure, exploration, long-term and real-time monitoring, and performing of various underwater missions. Herewith, tasks measuring the parameters of fields with precise navigational referencing, 3D visualization of surveying results, bathymetry, magnetometry, and gravimetry of different marine areas are relevant for practical applications.

Prospects of using AUVs for geophysical measurements at sea repeatedly served as subjects of research and development over the number of years. Originally this topic was

---

* Corresponding author: imtp@marine.febras.ru

raised in the monograph [1] and concerned the estimation of advantages, which can be introduced using AUVs. Later, similar problems were discussed in the works of Russian [2-17] and non-Russian specialists [18-22].

Bathymetry measurements always accompany echo-ranging surveys of the sea bottom terrain, usually performed using modern side-scan sonars, interferometric and multi-beam sonars, and synthetic aperture sonars.

Studying marine geomagnetic fields and its anomalies and solving magnetized object search and detection tasks are carried out using highly sensitive field-level meters and gradiometers. Some issues of solving search tasks utilizing AUVs equipped with magnetic anomalies meters were considered in works [1-6, 10].

The use of AUVs seems promising for trajectory measurements and mapping of local gravity fields or gravity anomalies (GA) with the prospect of using the results for navigation purposes.

An important tool, along with the creation of equipment and conducting field tests, is the development and research of information and computational models [23-24] of specific processes for measuring geophysical fields, their recording and mapping, including models for the use of AUV and the use of mission results. Gravimetric computational models and their capabilities in solving navigational adjustments tasks were studied in research [12-17].

Problems of mapping geophysical fields using AUV are essential by itself, and besides that are directly related to the solving tasks of navigation by distinctive GPF elements. These tasks may include the follows:

- search for the position of a fragment of the field map, recorded during the AUV movement, on the field reference map, which is related to the task of matching the fragment to the reference field;
- the best approximation of the field map in terms of accuracy of navigation for economical storage of the reference field onboard the AUV;
- estimating the informativeness of the field and developing the most meaningful route, i.e., the best route in terms of the accuracy of navigation by the GFP while moving along the route [25, 26].

Let's take a closer look at possible solutions to this kind of task.

2. SEARCH TASKS DURING MAPPING AND RECONSTRUCTING THE MAP OF ANOMALOUS GEOPHYSICAL FIELD BASED ON TRAJECTORY MEASUREMENTS FROM AUV

Let $F(x, y)$ be the function describing the cross-section of the field in a coordinate plane (x, y),, which can be denoted by the isoline map $F(x, y) = const$. The field meter, while moving alongside the trajectory, records a representation of the field $f(t)$ with some random error $\xi(t)$:

$$f(t) = F(x(t), y(t)) + \xi(t). \tag{2.1}$$

Suppose that coordinates (x, y) and projections of the speed vector (v_x, v_y) of the AUV (field meter) are given by an internal navigation system (INS) with errors $(\Delta x_a, \Delta y_a), (\Delta v_x, \Delta v_y)$. Then, coordinates $(x(t), y(t))$ related to the measurement of $f(t)$ differs from true ones

$$\tilde{x}(t) = x(t) + \Delta x_a + \Delta v_x t, \quad \tilde{y}(t)) = y(t) + \Delta y_a + \Delta v_y t. \tag{2.2}$$

Let's denote the field's measure of the variability alongside the trajectory by the value of field gradient $|\nabla F|$ or an increment $\Delta F = |\nabla F| v \, \Delta t$, where v is the moving velocity, Δt is the time interval.

The following interrelated tasks are of practical interest:

Task 1 consists of recovery of the field $F(x, y)$ map in the form of an intensity matrix, defined on the regular orthogonal grid, or as a set of isolines. The recovery of the field map must be performed by covering the given area by the net of trajectories and measurements (2.1) of the field with referencing to points (2.2.) obtained by inaccurate navigational data.

As usual, the control of an underwater robot consists of an assignment and correction of a navigational program in characteristic points (x_k, y_k) of the trajectory. The points can be derived from conditions of passing the field local extremums or condition of maximal field gradient:

$$\left\{ F(x_k, y_k) \equiv F_{max}^{loc} \;\|\; F(x_k, y_k) \equiv F_{min}^{loc} \,\|\, \left|\nabla F\right| \equiv \left|\nabla F_{max}^{loc}\right| \right\}. \qquad (2.3)$$

Task 2 consists of the search of field anomalies, which appear in the function F as areas of local extremums. For that, it is necessary to arrange a search motion trajectory for an underwater robot for detection and contouring the anomaly by the fixed level $F(t)$ and variability $\left|\Delta F(t)\right|$ of the field meter signal under the masking influence of external noises.

The search of coordinates with specific (extremal in particular) values the field parameters is vital for the determination of purposed motion cue. The search procedure can be performed based on orthogonal or gradient descent with an orientation towards a chosen target, such as an anomaly source. Accumulation of the data about the extremal values of the field allows outlining the borders of anomaly or boundaries of area (background) with no anomalies.

Task 3 is connected with tracking the given isoline $F(x, y) = const$, delimiting the boundaries of the anomaly by the given (extremal) field value. The motion is then organized by the orientation of the speed vector by the field behavior proportional to the value $\nabla F_x / \nabla F_y$. Generally, the search mission scenario includes the following processes:

- approaching the area with the given field level using orthogonal tacks and course correction according to field gradient sign;
- covering the fount area by the net of squarewave like rectilinear trajectories (tacks) with continuous measurements of the field parameters and mapping them to navigational data for further reconstruction of the field map;
- performing search movements by orthogonal descent for determination of the probable position of the extremum;
- tracking the given isoline delimiting the boundaries of the anomaly by pointing the speed vector according to the "curvature" of the field alteration or moving by calculated coordinates, which corresponds to the given field level.

The primary scenario process consists is a restoration of the field map be the net of discrete measurements obtained by covering the target area by rectilinear trajectories (tacks). Measured in nodes of the irregular net values are then interpolated with step depending on the value of the field gradient value in nodes. Based on obtained data, isolines with given values of the field can be created.

Motion control in the field of anomaly is a unique but yet practically important case. While developing the particular algorithms of AUV motion control during field anomaly investigation, it is necessary to consider features of the spatial structure of the field, including the presence of the natural background field, time and spatial distortions, and significant nonlinearities in their formal description. Examples of modeling the search motions and restoration of the map of investigating areas of the field are presented in [7-9, 11].

3. FEATURES OF THE VISUAL REPRESENTATION OF GEOPHYSICAL INFORMATION AND RESULTS OF ITS COMPREHENSIVE PROCESSING

As was mentioned before, the idea of using AUV for solving tasks of marine geodesy and navigation appeared at the very beginning of their development and then continuously evolved in theoretical and applied studies. Let's consider some of the results of research and computational experiments in the field of marine gravimetry.

First of all, it is worth mentioning that AUV is a well-stabilized platform abled of compensating external forces' actions, such as vertical accelerations of the carrier [2-4, 7-9]. Examples of gravimeter signal records obtained by AUV "Tiflonus" when working on the depth of 70 m are shown in the work [14].

The procedure of recording and restoration of the map of the gravity anomalies (GA) field based on trajectory measurements while covering the given area by a planned grid of trajectories with predetermined measurement accuracy are illustrated in Fig. 3.1. Here, particular estimations use a geographical map of residual gravity anomalies in the the Peter the Great Gulf, obtained in the Laboratory of Gravimetry of the V.I. Il'ichev Pacific Oceanological Institute (POI) FEB RAS using shipboard precision gravimetry Chekan-AM made by CSRI Elektropribor [10]. The map contains a selected fragment, which has a ceased volcano with a volatile GA gradient in the lower part of it (Fig. 3.1,a). A 50x40 km part of the field in this area was investigated using squarewave-like trajectories (Fig. 3.1,b). The computational experiment assumed that the processing time of the small tack is 20 min, which equals to the distance of 1.2 km on the speed of 1 m/s. Correspondingly, the processing time of the big tack is 14 hours, and the distance is 50 km.

Trajectories were created considering AUV dynamics in modes of depth and heading control. Obtained digital data then were used for the restoration of the field map using scripts of matrix transformation and functions of interpolation for 2D and 3D images (Fig. 3.1,b,c).
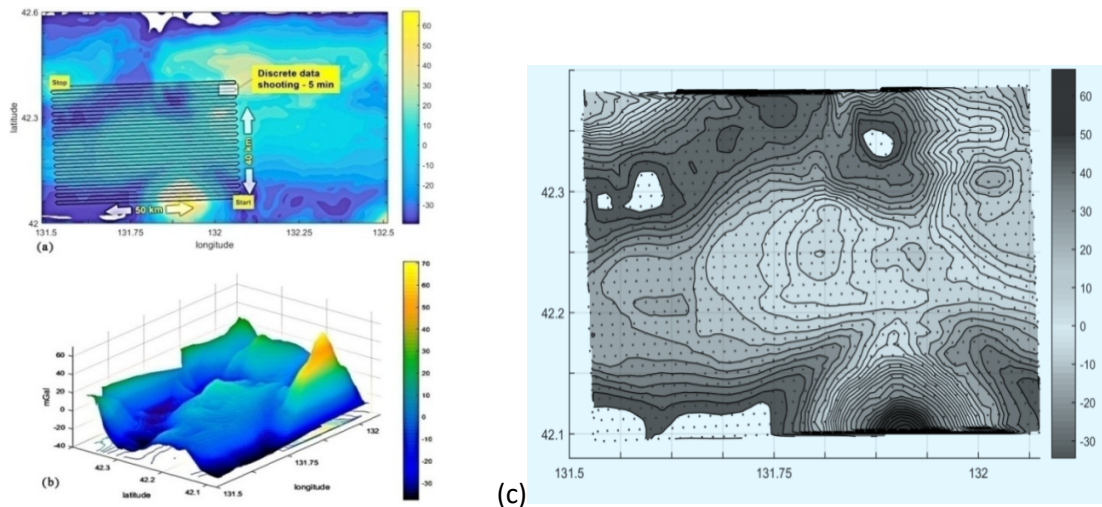
Fig. 3.1. The fragment of the GA geographical map with plotted squarewave-like trajectories (a); the 3D image of the recovered field fragment (b); a horizontal slice of the GA map recovered fragment (c)

A subject of undoubted interest is extensive use of all the available geophysical information, including bathymetry, magnetometry, and gravimetry. It allows firstly to find a possible correlation in measurements of heterogeneous fields, and secondly to obtain more certain and precise data for navigational correction by the cumulative results of mapping.

Let's have a closer look at the possibility of such an approach on the example of combining the data of mapping of sea depth field, geomagnetic field, GA field for the predetermined aquatic area. We will use an integrated mapping data for the studied area of the Strait of Tartary provided by the Laboratories of Gravimetry and Magnetometry of the FEB RAS. These initial maps originate from the expedition using high-precision shipboard


measurement devices. There are no similar available maps obtained with the help of AUV. Therefore, real maps are used, on which it can work out all the procedures simulating the trajectory measurements results of the field from the board of AUV. Recovered maps are virtual maps obtained using computational procedures based on the achievable results of trajectory measurements from the AUV, taking into account methodological errors (model errors) and measurement errors. These maps are actually analogs of those maps that can be obtained by using of AUV in real work. Further these maps are used as a reference ones to evaluate the accuracy of navigation by the GFP of certain moving objects, in the structure of which the map data is embedded. In the accepted computational model these maps are used to work out the evaluation algorithm described below. The initial 2D maps of these three fields are demonstrated in Fig. 3.2,a,b,c, and the reconstructed maps on Fig. 3.2,d,e,f.

Two-dimensional images of three fields shown in Fig. 3.2 can be transformed into 3D images in the form of corresponding reliefs of the spatial structure (an example of it can be fount in Fig. 3.1,b). Additional capabilities of the visual representation in the form of three-dimensional images can be obtained by a combination of the GA field, anomalous geomagnetic field (AGMF), and the sea depth field (SDF). Here, the sea depths axis is a vertical coordinate, and the other two form a projections of their 3D images on the upper (zero) level of the sea terrain field. Such representation can be got in the form of images obtained from any angle and any step of the image rotation angle. Note that according to the bathymetry matrix, the average depth of the selected area in the Tatar Strait is 2737 m.

Fig. 3.3 demonstrates examples of this visual representation with the covering the entire zone with squarewave-like trajectories when AUV is in motion on the depth of 1000 m. During movement along a given trajectory, simultaneous and spatially combined measurements of three fields are made.
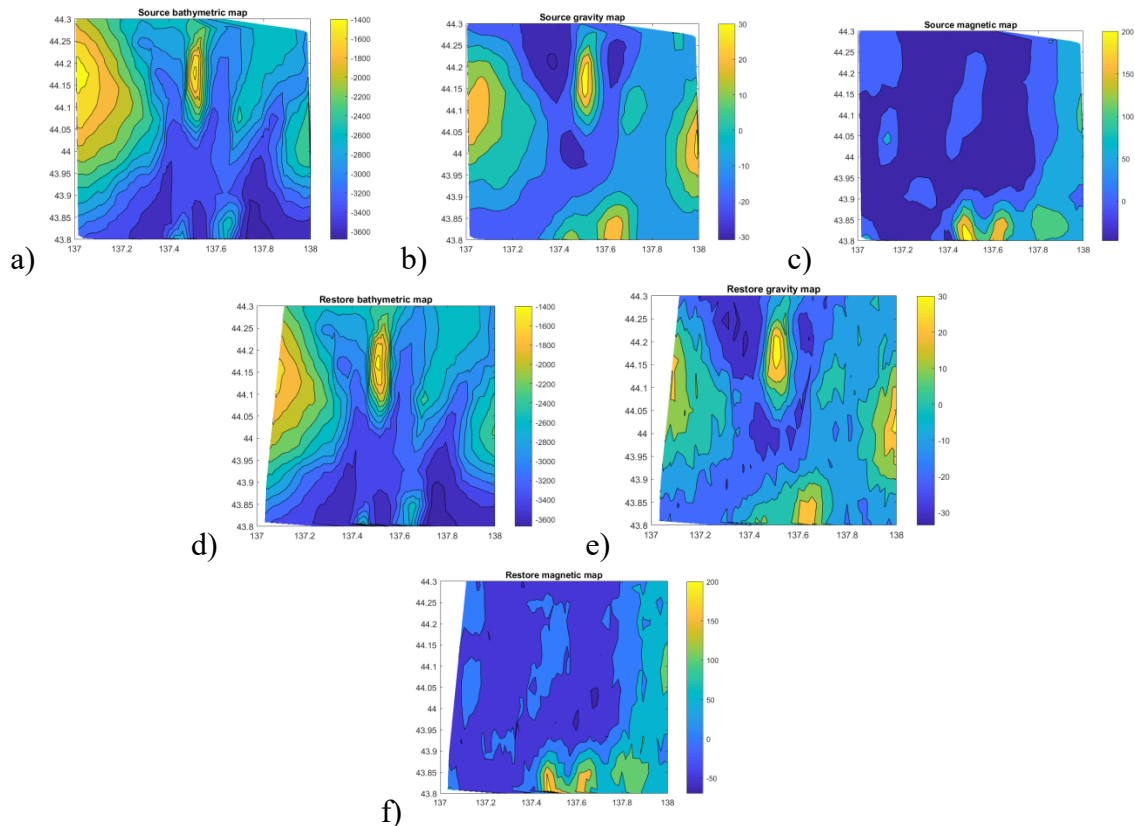
Fig. 3.2. Fragments of the initial maps of the sea depths (a), GA field (b), AGMF (c), map of the recovered fragmets of the sea depths field (d), GA field (e), AGMF (f)
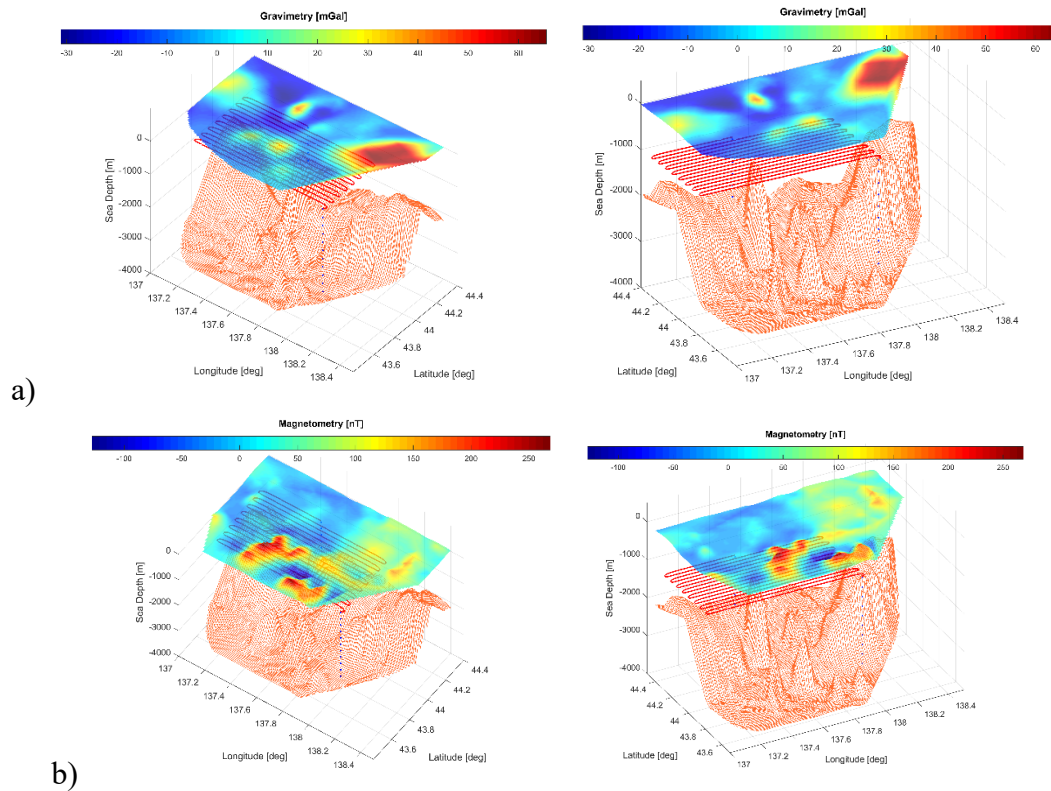
Fig. 3.3. Examples of the angle pictures combining the sea bottom's terrain field with GA field (a) and with the field of magnetic anomalies (b). The Redline shows the coverage trajectory. The images are obtained using Matlab graphic toolkit (functions surf(), mesh(), plot3()), where one space unifies data about physical fields of two types and trajectories with different color schemes (colormap())

4. ESTIMATION OF THE NAVIGATIONAL INFORMATIVENESS OF AN ANOMALOUS GEOPHYSICAL FIELD

Works [10-16, 27-29] consider issues of the informativeness of the anomalous GA field and estimating the accuracy of navigational correction by recovered field map.

Here the estimations of navigational informativeness of the fields (SDF, GA fields, and AGMF) recorded in the Tatar strait are considered.

Thereunder, the method of estimation of errors of map-aided navigation [32-35] proposed in [30, 31] is studied by the example of the joint using of three geophysical fields.

The task of the method of map-aided navigation is correction of errors of required navigational parameters (for example, coordinates (latitude and longitude) of the carrier) by the matching the measured field fragment to the reference map [33, 34, 36, 37]. The matching of the fragment and the reference map can be performed using the search of the global extremum of some *matching functional* of measured fragment and reference fragments obtained from the reference map.

The navigational informativeness of the geophysical field is measured by the level of navigation errors when using this method. As a rule, the main source of errors is misclosures of mapmaking and errors in field measurements while the object is moving. However, the sensibility of the navigation results to these errors is mainly determined by the gradient characteristics of the field itself.

Here, the task is considered in the probabilistic statement, as in works [33-35].

4.1. Theoretical estimation of errors of coordinates correction by the maps of geophysical fields

Since the map-aided method of navigation is used for the correction of errors of inertial navigation system, the task the navigation by geophysical field is often called the correction task of navigation system. Here, the task of coordinates error correction in a horizontal plane is considered.

Let's denote the reference map of the geophysical field defined in a certain rectangular area Ω of the plane R^2 ($\boldsymbol{x} = x_1, x_2$). by $g(\boldsymbol{x})$. Formally, the field map is a smooth function $g(\boldsymbol{x})$ of the two-dimensional vector $\boldsymbol{x}$ with values on the axis of real numbers.

Practically, the function $g(\boldsymbol{x})$ is represented by samples in nodes of a regular 2D grid with a given step size. If necessary, the values of the function $g(\cdot)$ between the nodes can be obtained using a proper interpolation method, for example, bilinear interpolation [38, pp. 123-128].

Let's consider that measurements of the field are performed in points of a rectilinear interval, which begins in the unknown point $\boldsymbol{x}$ in a given fixed direction defined by a unit vector $\boldsymbol{p}$. The model of the field measurement onboard the moving object can be expressed as:

$$\varphi_k \triangleq \varphi_x(t_k) = g(\boldsymbol{x} + t_k \boldsymbol{p}) + \xi_k, \ \ \boldsymbol{x} \in Q, \ k = 1,...m, \tag{4.1}$$

where φ_k is the value of the geophysical field measured in the discrete moment t_k. Then, let's denote the set of values (m-vector) $\boldsymbol{\varphi} = (\varphi_1,...\varphi_m)^T$ by a measured fragment of the field g or just a fragment.

The expression (4.1) consists of the following notions:

- $Q \subset \Omega$ is an area of a priori location of the initial point $\boldsymbol{x} \in Q$ of the fragment $\boldsymbol{\varphi}$ in the area Ω of the given reference map g;
- $\boldsymbol{x}$ is the actual location of the fragment;
- $\boldsymbol{p}$ is a given directing unit vector of the measurement route;
- $\boldsymbol{\xi} = (\xi_1,...\xi_m)$ is a vector of the fragment distortion.

Equality (4.1) can be rewritten in the vector form as:

$$\boldsymbol{\varphi} = \boldsymbol{s}(\boldsymbol{x}) + \boldsymbol{\xi}, \tag{4.2}$$

where m-vector $\boldsymbol{s(x)}$ is a set of samples recorded from the field map in time points t_k:

$$\boldsymbol{s}(\boldsymbol{x}) = (g(\boldsymbol{x} + t_1 \boldsymbol{p}),...g(\boldsymbol{x} + t_m \boldsymbol{p}))^T. \tag{4.3}$$

At its simplest, the vector $\boldsymbol{\xi}$ is a centered Gaussian vector with a zero mean and covariance matrix $\sigma_\xi^2 \boldsymbol{I}$ (where $\boldsymbol{I}$ is an identity matrix, σ_ξ^2 is a given dispersion). In reality, the distortion of the fragment along with the field meter random noises include the inaccuracies of mapping and errors of the relative positions of measurement points, which are caused by navigational errors of the carrier.

In the correction task, it is required to obtain the best estimation $\tilde{x}(\boldsymbol{\varphi})$ of the unknown vector $\boldsymbol{x}$ using given initial data and evaluate the accuracy of this estimation, for example, using the covariance matrix $P(\boldsymbol{\varphi})$.

In the framework of the Bayesian method, vectors $\boldsymbol{x}$ and $\boldsymbol{\xi} = (\xi_1,...\xi_m)$ are assumed to be random vectors with known distribution $f_x(\boldsymbol{x})$, $f_\xi(\boldsymbol{\xi})$.

Here, the main research subject is a correlation-extremal search method of the navigational error correction [24-26], which is added with the new approach for the correction error estimation based on the analysis of matching functional.

Let's consider the following quadratic functional of matching measurements and field map as an example:

$$\Phi(x) = \sum_{k=1}^{m}\left[g(x + t_k p) - \varphi_k\right]^2 \tag{4.4}$$

In this case, the estimation $\tilde{x}(\varphi)$ can be found as a result of the search of minimum:

$$\Phi(x): \tilde{x}(\varphi) = \arg\min_{x \in Q} \Phi(x) \tag{4.5}$$

The calculation of the correction error estimation relies on the following inequality:

$$\frac{\Phi(x_{min\_1})}{\Phi(x_{min\_2})} < P_{tr}, \tag{4.6}$$

where x_{min_1} is a point of the global minimum, x_{min_2} is a point of the second-biggest local minimum spaced apart from the first minimum x_{min_1} on a significant distance, P_{tr} is a threshold value. In the case of a single extremum, it is possible as $\Phi(x_{min\_2})$ take the minimum value of the functional at the boundary of the uncertainty domain. Inequality (4.6) shows how strongly the global minimum in (4.5) is pronounced against other local minimums, as the smaller the relation in (4.6), the more reliably the correction problem is solved in errors presence. In this context, this inequality describes the informativeness of the field in the Q. The threshold P_{tr} is derived from a statistical experiment using the Neumann-Pearson criterion and corresponds to the minimal level of the errors of the second kind at a fixed level of the errors of the first kind. Here the errors of the first kind are understood to be taking a wrong algorithm result as an accurate correction, and the errors of the second kind are understood to be a false rejection of the correction while the algorithm result is correct. In a statistical experiment, the correctness of algorithm output was defined by exceeding a predetermined threshold of the distance between the actual location of the fragment and the solution of the task (4.5).

At a predetermined threshold P_{tr}, it is possible to calculate the threshold $\Phi_{tr} = \dfrac{\Phi(x_{min\_1})}{P_{tr}}$

and then to find a diameter of the next set:

$$D_{max} = diam\{x : \Phi(x) \leq \Phi_{tr}\}. \tag{4.7}$$

In this case, the diameter of the set is defined as the maximum distance between the points of the set.

Thus, the result of the correction algorithm is taken as an estimate $\tilde{x}(\varphi)$ (4.5), and the value D_{max} (4.7) serves as an estimate error of the search algorithm, which can be calculated during the process work of the algorithm in real time without knowing the actual position x. In this case, the value of $\rho_{max} = D_{max}/2$ is an estimate of the maximum possible radial error of the correction.

Upon the availability of several spatially connected maps of different geophysical fields and a possibility of simultaneous measurement of these fields during motion, it is possible to co-use them to improve the accuracy of navigational error correction using a search algorithm (4.5). To do so, we will consider the matching functional $\Phi(x)$ of the following form:

$$\Phi(x) = \sum_{i=1}^{K}\alpha_i\left(\sum_{k=1}^{m}\left[g_i(x + t_k p) - \varphi_k^i\right]^2\right). \tag{4.8}$$

where K is a number of used geophysical fields, g_i is a map of the i-th field, φ_k^i is the k-th sample of the measured fragment of the ith field, α_i is a weight influence coefficient of the measurements of the i-th field on the matching functional.

Further coefficients α Coefficients α_i are accepted to be equal to inverse values of dispersions σ_i^2 of summary errors of the measurement and the reference map:

$$\alpha_i = (\sigma_i^2)^{-1}. \tag{4.9}$$

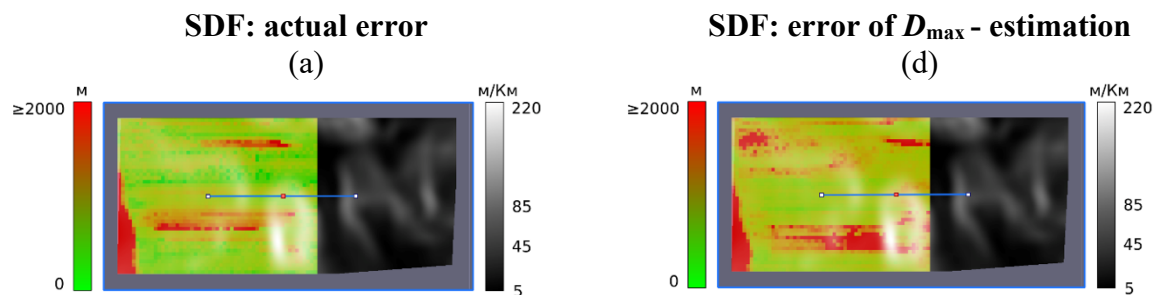### 4.2. Results of computational experiments

The most accurate and practically usable method of assessing the informativeness of geophysical field maps is a method of statistical imitational modeling of the process of navigational error correction, including repeated forming the sequence of measurements and their referencing to the reference field maps. Recovered maps of three fields recorded in the Tatar strait in coordinates E137º…E138º, N43,8º...N44,3º (Fig. 3.2,d-f) were used as reference maps. Maps were developed as matrices of samples assigned in nodes of the regular net with a step of 0.001° on both axes. Herewith, experiments involved forming of model measurements of the field by the initial maps of corresponding fields.
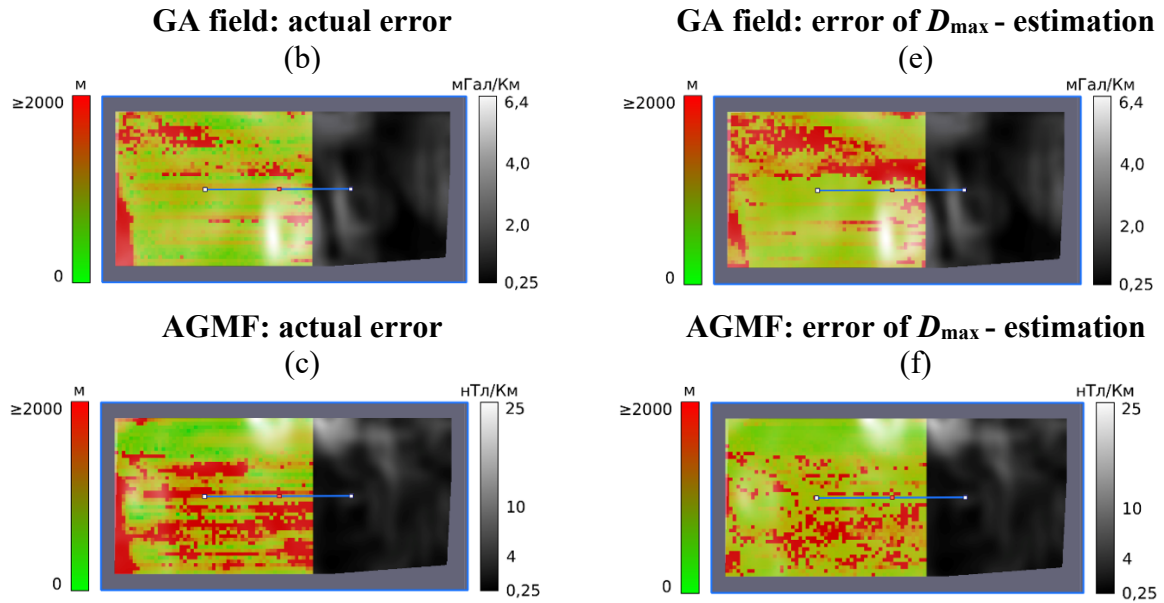
Experimental conditions

In correction zones for every three fields (their maps can be found in Fig. 3.2), we perform the forming of the model measurements of fields with the step of 100 m alongside rectilinear routes of 40 km directed along an X-axis. The correction was made by the recovered maps, shown in Fig. 3.2,d,e,f. Confidence rectangle Q (i.e., an area of the a priori location of the route beginning point, where a search of the functional minimum was performed (4.5)) had a size of 48x55 km. The size of the researched zones was approximately 85×55 km. The grid of the experiment containing the nodes, where the measurement paths began, covered the confidence rectangle with a step of 0.01 degrees (about 1 km). There were $N_э = 2880$ total experiments of correlation-extremal correction of navigation errors performed for each map. In each experiment, a set of measurements was modeled on the initial map, and the functional was formed (4.4) or (4.8) based on the reconstructed maps, the search for the functional minimum and the calculation of the radial D_{max} -estimate were performed.

The full generation model of the measurements of the SDF, GA field, and AGMF included errors of autonomous navigation, random errors of the meters: echosounder, gravimeter, magnetometer correspondingly. The approach for error generation of the GA field measurements and inertial navigation system is provided in work [14].

Fig. 4.1 comparatively demonstrates the results of statistical experiments of modeling the correction and obtaining the estimation of correction errors D_{max}. The results in Fig. 4.1 have the form of matrices with a size of 55×85 according to the grid in increments of one kilometer covering the research area. Herewith, GA field experiments specified the RMS deviation of the fluctuating part of the measurement error $\sigma_\xi = 3$ *mGal*, the computational threshold of the estimation D_{max} was chosen to be $P_{tr} = 0.8$. For the SDF, these parameters were taken equal to $\sigma_\xi = 60$ m, $P_{tr} = 0.6$. And for the magnetic field, they were equal to $\sigma_\xi = 7$ nT, $P_{tr} = 0.9$.

SDF: actual error
(a)

SDF: error of D_{max} - estimation
(d)

GA field: actual error
(b)

GA field: error of D_{max} - estimation
(e)

AGMF: actual error
(c)

AGMF: error of D_{max} - estimation
(f)

Fig. 4.1. A comparison between distributions of actual errors along the correction zone (a,b,c) and estimations using D_{max} (d,e,f). The predetermined green-red color scale (the scale is shown on the left in each figure) shows the values of the actual radial errors of coordinate correction and their D_{max}-estimations related to the initial points of the measurement routes located in the nodes of the kilometer grid. One of the measurement routes is shown in the center of every figure. All distributions are shown against the background of the corresponding halftone images, which represent the average radial modulus of the gradient of the study area in the gray scale (on the right). All the matrices shown in the figures correspond to the 85×55 km zones of the experiments.

In the presented results, the estimation error vector $\boldsymbol{\delta} = \boldsymbol{x} - \tilde{\boldsymbol{x}}(\boldsymbol{\varphi})$ for convenience is brought to the scalar value – radial error $r(\boldsymbol{\delta}) = \sqrt{\delta_{x_1}^2 + \delta_{x_2}^2}$, where $\delta_{x_1}^2, \delta_{x_2}^2$ are the squares of the vector $\boldsymbol{\delta}$ coordinates.

Fig. 4.2 uses the same color map and shows distributions of the actual error of the comprehensive correction along with all three fields according to the algorithm (4.7) and distribution of the corresponding D_{max}-estimation with the threshold P_{tr}=0.8.

(a) Combining fields: actual error

(b) Conbining ields: D_{max}-estimations
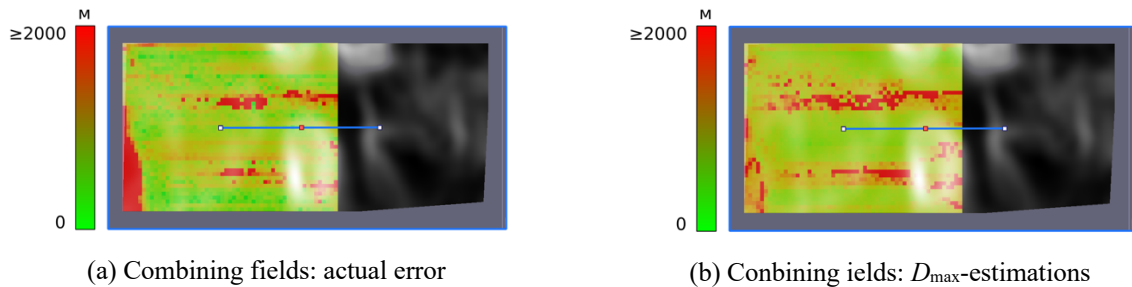
Fig. 4.2. A comparison between the distribution of the actual errors along the correction zones (a) and Dmax-estimation (b) when correcting by all three fields. The given colormap shows the values of coordinate correction errors and their Dmax-estimates related to the initial points of the measurement routes located in the nodes of the kilometer grid. One of the measurement routes is shown in the center of every figure.

The distributions of the errors are shown against the matrix of the integral informativeness, obtained by the weighted sum of the matrices of component fields.

The statistical mean values and statistical RMS of D_{max} - estimation (4.7) of the correction errors of the considered geophysical fields and their combination are shown in Table 4.1 in comparison with the actual errors for different locations $\boldsymbol{x} \in Q$ of the fragment ($N_{\ni} = 2880$) and for different RMS deviations of measurement errors $\boldsymbol{\xi}$.

Table 4.1. Results of a statistical experiment for the separate fields and their combination

	Correction by the GA field: $\sigma_\xi = 3$ mGal, $P_{tr} = 0.8$	Correction by the sea depths field: $\sigma_\xi = 60$ m, $P_{tr} = 0.6$	Correction by the magnetic anomalies field: $\sigma_\xi = 7$nT, $P_{tr} = 0.9$	Comprehensive correction by three fields: $P_{tr} = 0.8$
Actual error: $\bar{\delta}_S$ / RMS_S, m	980 / 811	761 / 752	1223 / 1015	671 / 737
Radial D_{max}- estimation: $\bar{\rho}_{max}$ / $RMS_{\rho_{max}}$, m	1300 / 837	1175 / 710	966 / 842	737 / 528

In the table, we accepted the following notations:

- $\bar{\delta}_S = \bar{r}(\tilde{x}_s(\boldsymbol{\varphi}) - \boldsymbol{x}) = \frac{1}{N_э} \sum_{i=1}^{N_э} r(\tilde{x}_s(\varphi_i) - x_i)$ - average actual radial error of the search algorithm, where $\tilde{x}_s(\varphi_i)$ – solution of task (4.5) in the i-th experiment, x_i – the actual position of the estimated parameter in the i-th experiment, $r(\cdot)$ - the expression described above;

- RMS_S – statistical standard deviation of the actual radial error $r(\tilde{x}_s(\varphi_i) - x)$ from its mean value;

- $\bar{\rho}_{max} = \frac{1}{N_э} \sum_{i=1}^{N_э} \rho_{max,i}$ - the average value of the error estimate of the search algorithm according to the method (4.7), где $\rho_{max,i}$ – where is the radial D_{max} - estimation in the i-th experiment;

- $RMS_{\rho_{max}}$ – statistical standard deviation of the radial D_{max} – estimation from its mean value.

Matching the results shown in Table 4.1 and distributions of the errors shown in Fig. 4.1, and Fig. 4.2 allow concluding that D_{max}-estimation is close to the actual estimation of the correction accuracy, which proves the applicability of the method for solving the tasks of this kind.

Regarding the navigational informativeness of considered geophysical fields, it is mentioning that the most informative (or the most accurate in terms of correction) field is an SDF, and the least informative is an AGMF. This actually shows the property of corresponding measuring systems and methods of measurement processing. It can be summarized that the complexing the measurements in three fields significantly increases the average accuracy of map-aided navigation: for the sea depths field of at least 10%, for the GA field of at least 30% and for anomalous geomagnetic field of at least 45%.

5. CONCLUSION

1. The preceding experience of works connected with the use of AUV for real-time and long-term monitoring of the geophysical fields of the ocean proves its viability for solving tasks of this kind. But on the other side, it demonstrated a number of theoretical and practical issues regarding the development of the proper computational models. These

models are based on methods of trajectory investigation of the areas and objects with respect to the features of the motion control tasks, information properties of the fields itself, and precision properties of the means of navigational correction by the recovered field map. Nowadays, gravimetry tasks are of particular importance thanks to the opportunity to perform it onboard the AUV, which is the precision stabilized platform with a minimum of the vertical accelerations. That establishes close relationships with tasks of inertial navigation. The results of natural and computational experiments show that this is a way for providing high-precision gravimetric measurements with the cumulative error of the GA field mapping of units of mGal, which corresponds to the geographical referencing error of units of meters.

2. Critical issues of the described research are:
- development of the models of trajectory investigation of the fields, anomalies search, and reconstruction of the map using the results of trajectory measurements;
- visual representation of the recovered fragments of the map in 2D and 3D formats and estimate the map reconstruction's accuracy regarding the dynamic errors, measurement, and navigation errors;
- development of computational models for estimating the information properties of reconstructed fragments of the field map for solving the task of navigational correction using a map-aided navigation approach.

3. Accuracy evaluation of correlation-extreme correction by the maps of geophysical fields is considered using specially developed a new method, which does not impose excessive requirements for onboard computer.

4. One of the main advantages of AUV equipped with the complex of meters of the geophysical fields is the joint processing of all the available information for the mapping and following use of it for navigational correction. Using software processing and 2D and 3D visual representation of digital formats, it is possible to find a correlation in the fields' scalar-vector properties, which can be an additional means for developing more precise computational models of map-aided navigation.

REFERENCES

1. Ageev M.D., Kasatkin B.A., Kiselev L.V., Molokov Yu.G., Nikiforov V.V., Rylov N.I. (1981). *Avtomaticheskie podvodnye apparaty* [Automated underwater vehicles]. Leningrad: Sudostroenie, 223, [in Russian].

2. Ageev M.D. (1994). AUV – a precise platform for underwater gravity measurement. *Proc. Of IEEE OCEANS'94, Brest, France.*

3. Ageev M.D, Kiselev L.V., Matvienko Yu.V., etc. (2005) *Avtonomnye podvodnye roboty. Sistemy i tekhnologii [Autonomous underwater robots. Systems and technologies]*. Moscow: Nauka, 400, [in Russian].

4. Ageev M.D. (2009) Avtonomnyj podvodnyj apparat – ideal'naya precizionnaya platforma dlya podvodnyh gravimetricheskih izmerenij [Autonomous underwater vehicle – an ideal precise platform for underwatger gravimetric measurements]. *Podvodnye issledovaniya i robototekhnika [Underwater research and robotics]*, 1(7), 4-8, [in Russian].

5. Kiselev L.V. (2009) Upravlenie dvizheniem avtonomnogo podvodnogo robota pri traektornom obsledovanii fizicheskih polej okeana [Motion control of autonomous underwater robot during trajectory measurements of the oceans physical fields]. *Avtomatika i telemekhanika [Automatics and telemechanics]*, 4, 141-148, [in Russian].

6. Kiselev L.V. (2011) *Kod glubiny* [Depth code]. Vladivostok: Dal'nauka, 331, [in Russian].

7. Kiselev L.V., Medvedev A.V. (2011) Modeli dinamiki i algoritmy upravleniya dvizheniem avtonomnogo podvodnogo robota pri traektornom obsledovanii anomal' nyh fizicheskih polej [Dynamic models and motion control algorithms of the autonomous underwater robot during trajectory measurements of the physical fields]. *Podvodnye issledovaniya i robototekhnika [Underwater research and robotics]*, 1(11), 24-31, [in Russian].

8. Kiselev L.V. (2017) Prioritetnye zadachi podvodnoj robototekhniki v oblasti morskoj geodezii [Priority tasks of underwater robotics in the marine geodesy]. *Proc. Of the XI conf. «Analiticheskaya mekhanika,utojchivost' i upravlenie» [Proc. Of the XI conf. «Analytical mechanics, adaptability and control»]*, Kazan', Russia, 138-151, [in Russian].

9. Inzarcev A.V., Kiselev L.V., Kostenko V.V., Matvienko Yu.V, Pavin A.M.,Shcherbatyuk A.F. (2018) *Podvodnye robototekhnicheskie kompleksy: sistemy, tekhnologii, primeneniya [Underwater robotic complexes: systems, technologies, applications]*. Vladivostok: Dal'press, 368, [in Russian].

10. Peshekhonov V.G., Stepanov O.A., Avgustov L.I., etc. (2017) *Sovremennye metody i sredstva izmereniya parametrov gravitacionnogo polya zemli [Modern methods and tools of measuring the parameters of the earth's gravitational field.]*. CSRI Elektropribor, ITMO university. Pod obshchej red. V.G. Peshekhonova; nauch. Redaktor O.A. Stepanov. Sankt-Peterburg, [in Russian].

11. Kiselev L.V., Medvedev A.V., Hmel'kov D.B. (2017). O nekotoryh zadachah podvodnoj robototekhniki v oblasti morskoj geofiziki [About some tasks of underwater robotics in marine geophysics]. *Proc. Of the 7 conf. «Tekhnicheskie problemy osvoeniya Mirovogo okeana» [Proc. Of the 7 conf. «Technical problems of the development of the World ocean»]*, 386-393, [in Russian].

12. Kostousov V.B., Tarhanov A.E. (2017). Ocenka informativnosti geofizicheskogo polya s tochki zreniya korrelyacionno-ekstremal' noj navigacii [Estimates of the informativeness of geophisical field in perspectives of map-aided navigation]. *Proc. Of the 7 conf. «Tekhnicheskie problemy osvoeniya Mirovogo okeana» [Proc. Of the 7 conf. «Technical problems of the development of the World ocean»]*, 394-398, [in Russian].

13. Kiselev L.V., Medvedev A.V., Kostousov V.B., Tarkhanov A.E. (2017) Autonomous underwater robot as an ideal platform for marine gravity surveys. *Proc. Of the 24-th Saint Petersburg International Conference on Integrated Navigation Systems. CSRI «Elektropribor»*, 605-608.

14. Kiselev L.V., Kostousov V.B., Medvedev A.V., Tarhanov A.E. (2019). O gravimetrii s borta avtonomnogo podvodnogo robota i ocenkah eyo informativnosti dlya navigacii po karte [About gravimetry onboard the autonomous underwater robot and estimation of its applicability to map-aided navigation]. *Podvodnye issledovaniya i robototekhnika [Underwater research and robotics]*, 1(27), 21-30, [in Russian].

15. Vitalii I. Berdyshev_ Lev V. Kiselev, Victor B. Kostousov. (2018) Mapping Problems of Geophysical Fields in Ocean and Extremum Problems of Underwater Objects Navigation / IFAC Papers On Line 51-32, 189–194.

16. Kiselev L.V., Kostousov V.B. (2019) On Interrelation and Similarity in Solution of Navigation and Gravimetric Tasks in Underwater Robotics. *Proc. Of the 26-th Saint Petersburg Intern.Conf. Integrated Navigation Systems. CSRI "Elektropribor"*. 395-397.

17. Kiselev L.V., V.B.Kostousov, K.V. Dunaevskaya, A.E.Tarhanov. (2020) Ocenka oshibok korrelyacionno-ekstremal' noj navigacii po karte anomalij sily tyazhesti na osnove traektornyh izmerenij s borta avtonomnogo podvodnogo robota [Error estimation of map-aided navigation by the map of gravity anomalies based on

trajectory measurements onboard autonomous underwater robot]. *Podvodnye issledovaniya i robototekhnika [Underwater research and robotics],* 1(31), 13-20, [in Russian].

18. Zumberge M.A., Hildebrand J.A., Stevenson J.M. (1991) Submarine measurements of the Nevtonian gravitational constant // Physical review letters. Vol. 67. Iss. 22.

19. Zumberge M.A., Sasagawa G., Zimmerman R., Ridgway J. (2010) Autonomous Underwater Vehicles Borne Gravity Meter. Patent Application Pub.No.: US 2010/0153050 A1, Jun.17.

20. Zumberge M.A., Sasagawa G., Zimmerman R., Ridgway J. Patent No. US 2010/0153050, A1. (Jun.17, 2010) Autonomous Underwater Vehicles Borne Gravity Meter.

21. Kinsey J., Tivey M., Yoerger D. (2009) Toward High-Spatial Resolution Gravity Surveying of the Mid-Ocean Ridges with Autonomous Underwater Vehicles. WHOI Deep Ocean Exploration Institute and a WHOI Green Innovation Technology Award.

22. Melo J., Matos, A., (2017) Survey on advances on terrain based navigation for autonomous underwater vehicles, Ocean Engineering, vol. 139, 250–264.

23. Calder M *et al*. 2018 Computational modelling for decision-making: where, why, what, who and how. *R. Soc. Open sci.* **5**: 172096. http://dx.doi.org/10.1098/rsos.172096

24. GOST R 57412-2017 Komp'yuternye modeli v processah razrabotki, proizvodstva i ekspluatacii izdelij. Obshchie polozheniya (GOST R 57412-2017 Computer models of products in design, manufacturing and maintenance. General), [in Russian].

25. Stepanov O.A., Nosov A.S., Toropov A.B. (2018) Navigacionnaya informativnost' geofizicheskih polej i vybor traektorij v zadache utochneniya koordinat s ispol'zovaniem karty [Navigational informativeness of geophysical fields and trajectory selection in the problem of coordinate refinement using a map]. Proceedings of the Tula State University. Technical Sciences. № 5, 74-92, [in Russian].

26. Berdyshev V.I., Kostousov, V.B. (2007) *Ekstremal'nye zadachi i modeli navigacii po geofizicheskim polyam* [*Extreme problems and models of navigation in geophysical fields*]. Ekaterinburg: UB RAS, 2007. P. 270, [in Russian].

27. Zheleznyak L.K., Koneshov V.N. (2007) Izuchenie gravicionnogo polya Mirovogo okeana [Investigations of the gravitational field of the world ocean]. *Vestnik RAN*, 77(5), [in Russian].

28. Koneshov V.N., Nepoklonov V.B., Avgustov L.I. (2016) Ocenka navigacionnoj informativnosti anomal'nogo gravicionnogo polya zemli [Estimation of navigational informativeness of the earth's anomalous gravitational field]. Giroskopiya i navigaciya [Gyroscopy and Navigation]. T. 24. № 2 (93). 95-106, [in Russian].

29. Kopytenko YU.A., Petrova A.A., Avgustov L.I. (2017) Analiz informativnosti magnitnogo polya zemli dlya avtonomnoj korrelyacionno-ekstremal'noj navigacii [Analysis of the informativeness of the Earth's magnetic field for autonomous map-aided navigation]. *Fundamental and applied hydrophysics* [*Fundamental and applied astrophysics*]. T. 10. № 1. 61-67, [in Russian].

30. Kostousov V.B., Dunaevskaya K.V. (2018). Metod korrekcii navigacionnyh oshibok po polyu vysot ob "ektov mestnosti [Methods for navigation error correction using the field of terrain objects height field]. *Proc. Of the XXXI conf. In memoriam of N.N.Ostryakova*, 218-227, [in Russian].

31. Kostousov V.B., Tarhanov A.E. (2019) Novyj metod ocenki oshibok korrekcii koordinat po karte geofizicheskogo polya [New estimation method for coordinates error correction by the map o geophysical field]. *Proc. Of the 8 conf. «Tekhnicheskie*

problemy osvoeniya Mirovogo okeana» [Proc. Of the 8 conf. «Technical problems of the development of the World ocean»]. 347-351, [in Russian].

32. Beloglazov I.N., Dzhandzhgava G.I., Chigin G.P. (1985). *Osnovy navigacii po geofizicheskim polyam* [Basic of navigation by the physical fields]. Moscow: «Nauka», 328, [in Russian].

33. Stepanov, O.A, Toropov, A.B.: Nonlinear filtering for map-aided navigation, part 1: An overview of algorithms. Gyroscopy and Navigation, 6(4):324–337 (2015)

34. Stepanov, O.A, Toropov, A.B.: Nonlinear filtering for map-aided navigation, part 2: Trends in the algorithm development. Gyroscopy and Navigation, 7(1):82–89 (2016)

35. Stepanov O.A. (2017). *Osnovy teorii ocenivaniya s prilozheniyami k zadacham obrabotki navigacionnoj informacii. Chast' 1. Vvedenie v teoriyu ocenivaniya* [Basics of estimation theory with applications to the tasks of navigational information processing. Part 1. Introduction to estimation theory]. Saint-Peterburg: CSRI «Elektropribor», [in Russian].

36. Stepanov O.A., Nosov A.S. A Map-Aided Navigation Algorithm without Preprocessing of Field Measurements Gyroscopy and Navigation, 2020, 11(2), 162–175.

37. Nosov, A.S., Stepanov, O.A. (2018) The effect of measurement preprocessing on the accuracy of map-aided navigation. 25th Saint Petersburg International Conference on Integrated Navigation Systems, ICINS 2018 - Proceedings, 1–4.

38. Press, William H.; Teukolsky, Saul A.; Vetterling, William T.; Flannery, Brian P. (1992) *Numerical recipes in C: the art of scientific computing* (2nd ed.). New York, NY, USA: Cambridge University Press.